General Application of the Relative Calibration Adjustment (RCA) Technique for Monitoring and Correcting Radar Reflectivity Calibration

DAVID B. WOLFF

NASA Wallops Flight Facility, Wallops Island, Virginia

DAVID A. MARKS

NASA Wallops Flight Facility, Wallops Island, Virginia, and Science Systems and Applications, Inc., Lanham, Maryland

WALTER A. PETERSEN

NASA Wallops Flight Facility, Wallops Island, Virginia

(Manuscript received 13 September 2013, in final form 20 October 2014)

ABSTRACT

Accurate calibration of radar reflectivity is integral to quantitative radar measurements of precipitation and a myriad of other radar-based applications. A statistical method was developed that utilizes the probability distribution of clutter area reflectivity near a stationary, ground-based radar to provide near-real-time estimates of the relative calibration of reflectivity data. The relative calibration adjustment (RCA) method provides a valuable, automated near-real-time tool for maintaining consistently calibrated radar data with relative calibration uncertainty of ±0.5 dB or better. The original application was to S-band data in a tropical oceanic location, where the stability of the method was thought to be related to the relatively mild ground clutter and limited anomalous propagation (AP). This study demonstrates, however, that the RCA technique is transferable to other S-band radars at locations with more intense ground clutter and AP. This is done using data from NASA's polarimetric (NPOL) surveillance radar data during the Iowa Flood Studies (IFloodS) Global Precipitation Measurement (GPM) field campaign during spring of 2013 and other deployments. Results indicate the RCA technique is well capable of monitoring the reflectivity calibration of NPOL, given proper generation of an areal clutter map. The main goal of this study is to generalize the RCA methodology for possible extension to other ground-based S-band surveillance radars and to show how it can be used both to monitor the reflectivity calibration and to correct previous data once an absolute calibration baseline is established.

1. Introduction

To improve the quality of the Tropical Rainfall Measuring Mission (TRMM) and Global Precipitation Measurement (GPM) ground validation (GV) rain maps being produced at NASA's Goddard Space Flight Center (GSFC), it was necessary to develop a means to calibrate current radar data and postcalibrate the 16-plus years of prior radar data from the oceanic GV site located on Kwajalein Atoll in the Republic of the Marshall Islands. Indeed, several previous attempts to postcalibrate the Kwajalein S-band dual-polarization radar (KPOL) were made using observations of solar radiation and standard targets (Atlas and Mossop 1960). However, unexpected sensitivity changes occurred on numerous occasions in KPOL reflectivity data that produced subsequent errors in the estimated rainfall. It was therefore necessary to find a means both to detect and to adjust such errors on a more routine and automated basis. Silberstein et al. (2008) presented the relative calibration adjustment (RCA) technique, based loosely on the method of Rinehart (1978), to monitor the calibration state of KPOL. The RCA approach utilizes the probability distribution of the clutter area reflectivity at a specified elevation during both rainy and rain-free days. The overall distribution of clutter area reflectivity can change significantly due to varying intensities of precipitation

Corresponding author address: David B. Wolff, NASA Wallops Flight Facility, Code 610.W, Building N-159, Room E214, Wallops Island, VA 23337.
E-mail: david.b.wolff@nasa.gov

DOI: 10.1175/JTECH-D-13-00185.1

TABLE 1. Attributes of the NPOL radar. Simultaneous transmit and receive (STAR).

NPOL attributes	
Transmitter type	Coaxial magnetron
Modulator type	Solid state
Operating frequency	2700–2900 MHz, tunable
Polarization	Horizontal and vertical, simultaneous/alternating
Peak pulse power output (STAR)	425 kW H, 425 kW V; typical
Peak pulse power output	850 kW, typical
Pulse width	0.8 or 2.0 μs, selectable
Beamwidth	0.98°
PRF	250–1200 s^{-1}
Duty cycle	0.001 maximum

TABLE 2. Description of fields recorded or processed by the NPOL radar system.

NPOL field types		
Field	Unit	Description
Z_T	dBZ	Total (unfiltered) reflectivity
Z_H	dBZ	Horizontal reflectivity (filtered)
Z_{DR}	dB	Differential reflectivity
Φ_{DP}	°	Differential phase
K_{DP}	° km^{-1}	Specific differential phase
ρ_{HV}		Copolar correlation
SQI		Signal quality index

coverage; however, the 95th percentile of the clutter distribution is remarkably stable in the absence of either pointing angle errors or engineering changes. As described in Silberstein et al. (2008), it is the stability in the top 95th percentile of clutter area reflectivity that allows the detection of relative calibration changes. Except for the case of echoes originating from wind-driven trees, echoes included in the RCA statistical analysis do not fluctuate. The calculation of the calibration adjustment factor is determined by comparison of the 95th percentile distribution to an established baseline, as is discussed later in the text.

A comprehensive review of the nature of ground clutter in a variety of environments is available in Skolnik (2001, chapter 7). Additional information on ground clutter can be found in papers by Billingsley and Larrabee (1991) and Billingsley (1993) as well as others in the Skolnik review. For present purposes it is sufficient to note that most significant clutter echoes at low angles come from spatially localized or discrete vertical features associated with elevated regions of the visible landscape (e.g., trees, buildings, or towers). The reader is referred to Skolnik (2001, his Table 7.1 and Figs. 7.4 and 7.5) for details on the typical strength of clutter echoes from various types of terrain as a function of wavelength.

Silberstein et al. (2008) examined the possible effects of anomalous propagation (AP) over relevant intervals from hours to months and found no significant variations. This was originally thought to be a benefit of the relatively quiescent oceanic tropical environment of Kwajalein; however, as shown herein, the RCA technique can be applied to NASA's dual-polarimetric (NPOL) S-band ground-based radar in a location with intense AP in the domain. A clutter map consisting of targets near the radar (nominally within 1–5 km) must first be carefully constructed. We demonstrate the stability of the RCA method using data collected by NPOL in a variety of AP and precipitation regimes from central Iowa during the Iowa Flood Studies (IFloodS) GPM GV field campaign in spring 2013. The method has also been successfully applied to NPOL data from the Midlatitude Continental Convective Clouds Experiment (MC3E; Jensen et al. 2010) and the Integrated Precipitation and Hydrology Experiment (IPHEx) GPM GV field campaigns in 2011 and 2014, respectively. The NPOL radar is described in Gerlach and Petersen (2011). Tables 1 and 2 provide details of the NPOL radar system and moments recorded.

Section 2 describes development of the clutter map and baseline statistics needed for RCA application. Section 3 describes NPOL radar operations and how the RCA method was applied to NPOL data from the IFloodS field campaign. The IFloodS RCA results are used in section 4 to demonstrate the efficacy of the tool for monitoring near-real-time calibration and to describe a straightforward method for absolute post-calibration of data. Section 5 provides two case studies illustrating how the RCA is able to detect radar system changes, including a subtle change in elevation angle. Conclusions are summarized in section 6 with a discussion of future applications of RCA to NPOL and potentially other radars.

2. RCA clutter map and baseline development

a. *Clutter map development*

The RCA is simply explained as a calibration adjustment applied to reflectivity data in order to obtain agreement to an established baseline. The adjustment is based on the 95th percentile of the clutter area reflectivity (Silberstein et al. 2008). A clutter map must first be developed to determine the statistical distribution of the clutter area reflectivity. To construct a clutter map for IFloodS, we selected a single precipitation-free day (2 June 2013), limited the area of interest from 1 to 5 km from the radar, and set a reflectivity threshold of 55 dBZ. The range is limited in order to avoid complications due to sidelobe and beam propagation effects. The selection

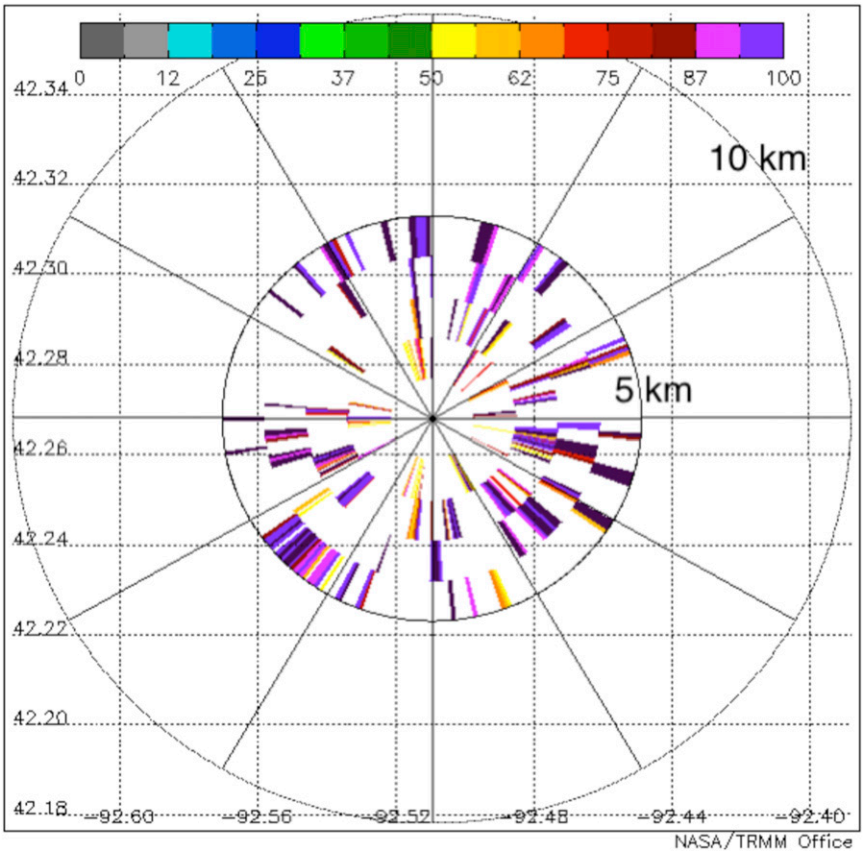

FIG. 1. Clutter map for the NPOL radar for the IFloodS field campaign. To construct the clutter map, we selected a single day (2 Jun 2013) that was precipitation free within 1–5 km of the radar. Colors represent the value of PCT_on at each clutter point. See section 2 for a discussion of clutter point selection.

of 55 dBZ is somewhat arbitrary in that the actual threshold must be greater than the bulk of precipitation base reflectivity values common to a particular regime, but not so large as to be above the common reflectivity values of nearby clutter targets. For example, a threshold of 50 dBZ for Kwajalein is much more appropriate than it would be for Iowa, where high reflectivity values associated with hail are more common.

The following steps are taken to develop the RCA clutter map.

1) Select all PPIs for a day with no precipitation within 5 km of the radar.
2) Create a fixed polar grid/array (FPG) with a resolution of 1 km × 1° to serve as a mask for constructing the clutter map, which itself will be an FPG array of the same resolution. Note that this is necessary because NPOL radar azimuth pointing angles are not fixed, and thus a coarser, fixed grid is more convenient.
3) Using the 1 km × 1° elements of the FPG array, flag each PPI pixel (i.e., reflectivity value at the radar-observed range and azimuth) that exceeds the specified threshold. A value of one indicates that at least one PPI pixel within the FPG element exceeded the threshold, while a value of zero means that no PPI pixels within the FPG element exceeded the threshold.
4) Save the FPG array and repeat for all PPIs for the given day.
5) Sum the saved FPG arrays and divide by the total number of PPI scans to obtain the percentage of occurrence that each of the FPG elements contained at least one pixel that exceeded the threshold [“percent on” (PCT_on)].
6) The final clutter map is then defined as the range and azimuth locations where PCT_on is ≥50%. All other elements are not designated as clutter points.

Figure 1 shows the clutter map for the NPOL radar for the IFloodS field campaign. The observed reflectivity values within the 1 km × 1° elements designated as clutter are hereafter referred to as the clutter area reflectivity.

b. Baseline development

After a clutter map has been constructed, the next step in calculating the RCA is to determine the baseline from which all relative calculations for other periods are compared. The baseline does not necessarily represent the actual *absolute* calibration of the radar reflectivity, but rather it is a benchmark from which RCA values for other days can be compared. Further, the obtained 95th percentile reflectivity is not "selected" but rather results from the character of the observed clutter area reflectivity.

The RCA technique collects the clutter area reflectivity for a given day and then computes the probability density function (PDF) and cumulative distribution function (CDF). The CDF is used to calculate the 95th percentile reflectivity. Once the 95th percentile reflectivity is calculated for a given day, the RCA is defined by Eq. (1):

$$\mathrm{RCA} = (\mathrm{dBZ95}_{\mathrm{baseline}} - \mathrm{dBZ95}_{\mathrm{daily}}), \qquad (1)$$

where $\mathrm{dB}Z95_{\mathrm{baseline}}$ is the 95th percentile baseline reflectivity and $\mathrm{dB}Z95_{\mathrm{daily}}$ is a specific daily 95th percentile clutter area reflectivity. By definition, the RCA value is the adjustment (dB) needed to obtain agreement to the baseline. A *positive* RCA infers that the radar is running *low* relative to the baseline, while a *negative* RCA infers that the radar is running *high* relative to the baseline.

Figure 2a provides the hourly and daily PDF and CDF of clutter area reflectivity from data observed on 2 June 2013. This plot shows hourly PDFs and CDFs, as well as the hourly RCA values (gray-scaled text on left). There was no precipitation on this day, so the hourly PDFs and CDFs are in close agreement. In contrast, note the behavior of the PDFs and CDFs in Fig. 2b, plotted for a date when significant precipitation did occur (4 May 2013). Hourly clutter area distributions show a large spread as a result of the influence of precipitation; however, the distributions converge by the 95th percentile, indicating the minimal influence of precipitation at the level used for calculation of the RCA. As explained in Silberstein et al. (2008), it is this attribute that allows the method to be applied to any day regardless of precipitation coverage.

3. IFloodS and NPOL operations

In the spring of 2013 (1 May–15 June), NASA, in collaboration with the University of Iowa, as well as other government agencies and members of the U.S. academic research community, conducted a field experiment in northeastern Iowa referred to as the Iowa Flood Studies. The main goal of the experiment was to support prelaunch integrated hydrologic ground validation activities of GPM. Specifically, IFloodS was designed to help quantify the physical characteristics and the space/time variability of precipitation, to assess satellite rainfall retrieval uncertainties at instantaneous to daily time scales, and to evaluate the propagation/impact of estimation uncertainties in flood prediction. In addition, primary goals included discerning the relative roles of rainfall quantities such as rain rate and accumulation as compared to other factors (e.g., transport of water in the drainage network) in flood genesis and refining GPM GV approaches to the "integrated hydrologic GV" concept based on IFloodS experiences.

The NPOL radar encountered few problems during the field campaign, so little to no data were lost during rainy periods. Over the span of the campaign, NPOL observed a myriad of events including snow and sleet (2–5 May 2013), rain, hail, strong convection with severe wind gusts, and an outbreak of tornadoes (12 June 2013). In addition, significant AP and double trip echo were observed. Thus, the IFloodS NPOL dataset provides a unique opportunity to determine the stability of the RCA technique in a variety of precipitation/echo regimes from the extreme to the mundane. The radar tasks during IFloodS consisted of high temporal frequency plan position indicator (PPI) rain scans, providing 360° coverage at low elevations, as well as PPI sector and range–height indicator (RHI) scans, dependent on the occurrence and location of precipitation echoes. Entire PPI–RHI scan cycles were completed in 1–3 min whenever precipitation was within range of the radar. When there were no precipitation echoes near the radar or over key areas in the domain, NPOL was operated in a two-sweep "surveillance" scan utilizing full PPIs.

We utilized only the lowest sweep of these PPI scans for developing, testing, and executing the RCA. The clutter map was constructed as described in section 2, and the RCA baseline was established using data from a day with no precipitation or AP (2 June 2013). Figure 3 shows the RCA daily time series for the IFloodS campaign. The legend at the top left indicates minimal variability of the daily RCA with a standard deviation of only 0.13 dB. What is remarkable is the relative smoothness of daily values, given the diverse weather that was observed during the campaign.

For the 2 June data, the minimal presence of AP was determined through visual observation of the radar data and by review of local and synoptic meteorological conditions. In general, extreme AP can be identified through examination of the dual-polarization data (low cross correlation ρ_{HV} and large variance of specific differential phase K_{DP}; not shown). For more information, see Ryzhkov and Zrnic (1998). An important question is

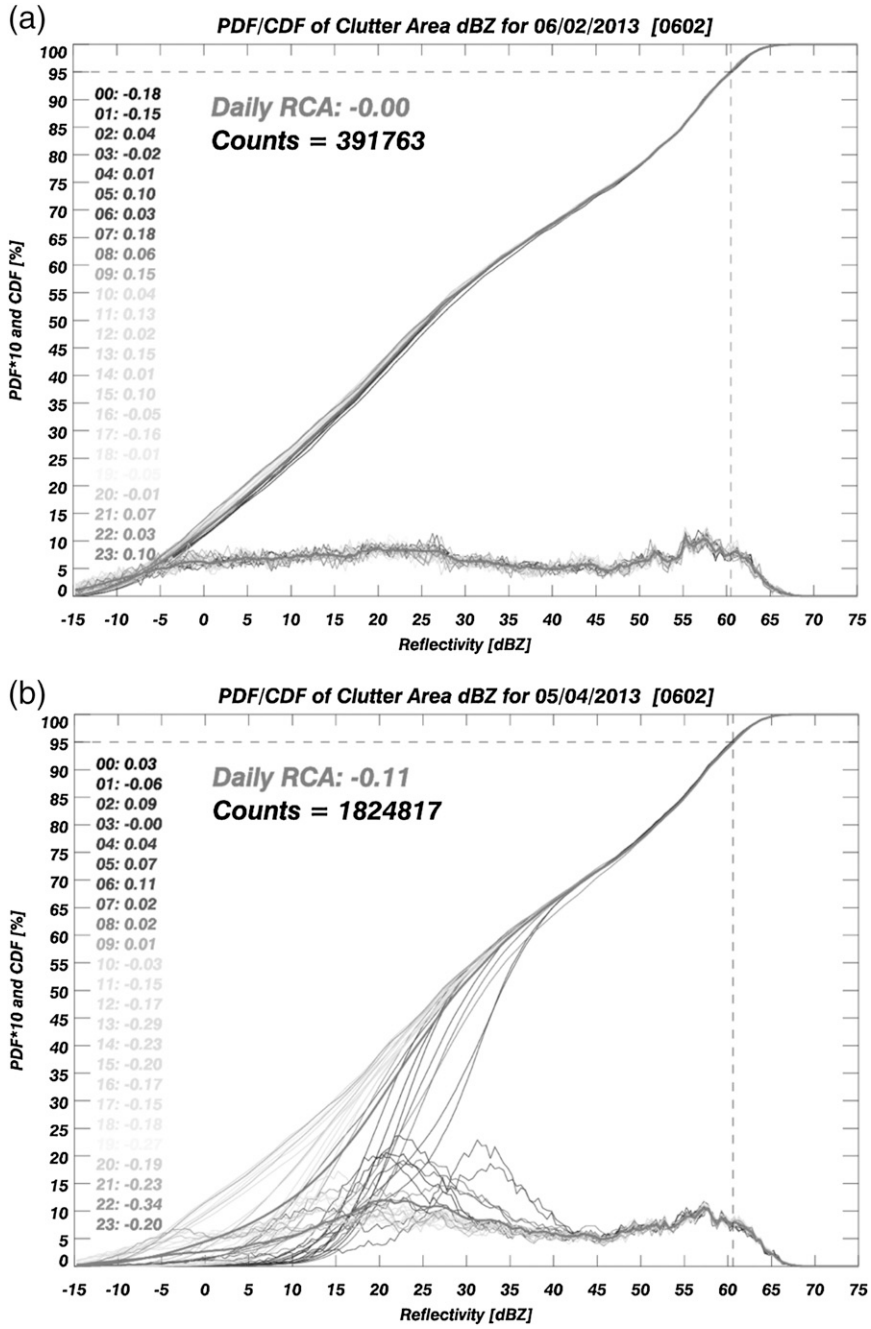

FIG. 2. (a) PDFs and CDFs of hourly clutter area reflectivity for NPOL on 2 Jun 2013. Data from this date were used to construct the clutter map and to select the baseline 95th percentile clutter area reflectivity for comparison with other days. This figure illustrates the stability of the distributions on an hourly basis (each PDF and CDF are grayscale coded by hour). The complete daily distribution is plotted as the bold gray line. The hourly RCAs are listed in the text on the left. (b) PDFs and CDFs from 4 May 2013, when widespread precipitation occurred over the entire radar domain. While the PDFs vary significantly in the lower percentiles (left side of graph), they converge nicely by the 95th percentile (intersection of the dashed horizontal and vertical lines).

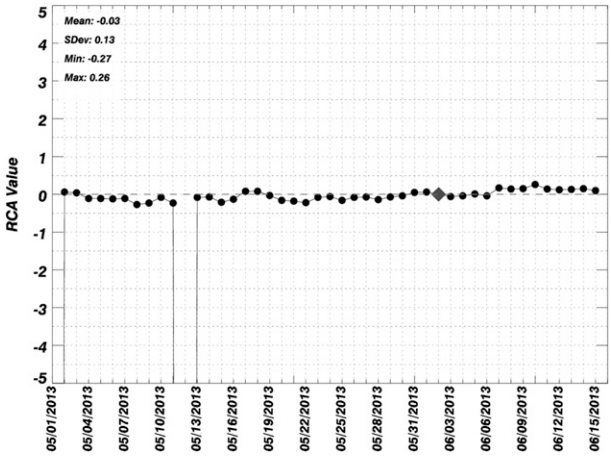

FIG. 3. Time series of daily RCA values for NPOL during IFloodS. The legend at the top left shows the mean, standard deviation, minimum, and maximum of the daily RCA values. The diamond represents the day (2 Jun 2013) from which the baseline RCA was derived.

then, how sensitive is the RCA to precipitation and AP within the clutter map area? The simple answers are 1) the rare precipitation echoes that occur in the clutter area are usually considerably lower than the 95th percentile reflectivity, so they have little effect on the upper end of the reflectivity distribution; and 2) it is quite rare that AP can be so strong as to ensconce areas within 1–5 km of the radar. By constructing the clutter map within this range, no significant AP is integrated into the RCA calculations. To demonstrate these points, we examined different "clutter map days" with the following echo characteristics: 1) predominant precipitation, little AP; 2) no precipitation, significant AP; and 3) no precipitation, little AP. By executing the RCA procedure over all data using these different clutter maps, we demonstrate how each effect propagates through the time series of the entire campaign. Table 3 provides a description of the days chosen to represent the characteristic echo events.

Figure 4a shows characteristic PPI images from the days listed in Table 3. These images are representative of predominant echo types observed on the given days. For example, Fig. 4a, panel 1, illustrates the light precipitation that occurred on 2 May 2013 that covered the region with reflectivity values on the order of 10–30 dBZ for most of the day. Figure 4a, panel 2, shows an extreme AP event that occurred on 16 May 2013 with echoes >30 dBZ occurring over a significant fraction of the radar domain. Finally, Fig. 4a, panel 3, shows a PPI from 2 June 2013 with no precipitation or AP, and light to moderate clutter observed in the first 50 km.

To demonstrate the relative insensitivity of the RCA retrievals to the chosen clutter map, panels 1–3 of Fig. 4b show the resultant campaign time series of daily RCA values when using the clutter map constructed from data observed on 2 and 16 May, and 2 June 2013, respectively. Table 4 lists the RCA statistics for these specific days and includes other days not shown in this paper. Results indicate that the method is largely insensitive to the chosen clutter map (i.e., insensitive to precipitation and AP), as long as the clutter map areas are restricted to ranges close to the radar, for example, 1–5 km.

To quantify the variability of the 95th percentile of clutter area reflectivity (dBZ95), we calculated the standard deviation of both the hourly and daily dBZ95 values over an entire month during IFloodS operations when no known engineering or other issues altered the reflectivity calibration. For May 2013, the mean dBZ95 was 60.59 dBZ, with hourly and daily standard deviations of 0.18 and 0.12 dB, respectively. Hourly and daily standard deviations were also computed for an entire month from both MC3E and IPHEx field campaigns (NPOL) and also the KPOL radar at Kwajalein with similar results (hourly standard deviations ≤0.3 dBZ for all three datasets.

4. Operational use of the RCA

In an operational sense, we do not fine-tune reflectivity values on a day-to-day basis when they are small (e.g., ±0.5 dB, given the inherent uncertainty of RCA values), but instead try to identify systematic changes, investigate their probable cause, and then adjust if deemed appropriate. Hence, we will refer to the actual variability as ±0.5dB for practical purposes, which is well below most expected accuracy inherent to any absolute calibration methods. If it is determined that a significant jump (>±0.5 dB) has occurred that is thought to be caused by a change in the radar calibration, then a manual adjustment to the data can be made. However, before an adjustment can be made in this manner, it is critical that an accurate estimate of the *absolute* calibration be made by independent means

TABLE 3. Dates chosen as example "clutter map" days and description of the predominant echo characteristics.

Date	Description
2 May 2013	Precipitation predominantly in clutter area (1–5-km range) but consisted of light stratiform rain. No significant AP.
16 May 2013	Major AP event. "Bloom" enveloped entire domain at times and lasted most of the day.
6 Jun 2013	Little precipitation present in clutter area (1–5-km range). No significant AP.

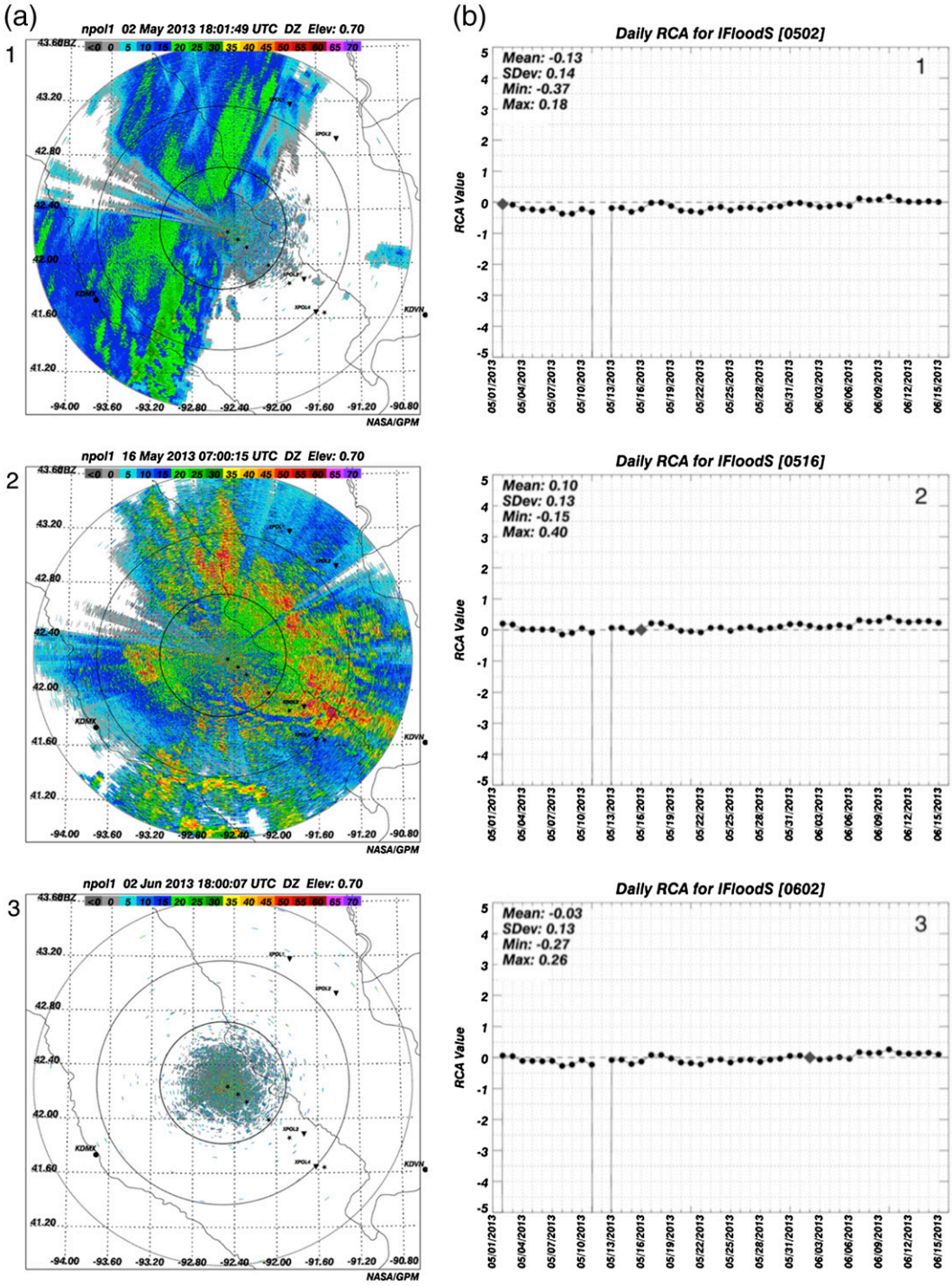

FIG. 4. (a) Representative PPI images from selected cases from IFloodS: (1) characterized by light precipitation over the radar for the bulk of the day on 2 May 2013; (2) extreme AP present on 16 May 2013; and (3) no precipitation, light AP day on 2 Jun 2013. (b) Time series of RCA retrievals when using the clutter map constructed from data observed for the dates illustrated in (a): (1) 2 May 2013, (2) 16 May 2013, and (3) 2 Jun 2013.

TABLE 4. Resultant statistics of RCA application using different days for the generation of clutter maps.

Date	Mean	Std dev	Min	Max	Echo characteristics
2 May 2013	−0.13	0.14	−0.37	0.18	Light reflectivity values associated with cold rain persisting radar most of day.
10 May 2013	0.06	0.14	−0.17	0.41	Light rain over radar early with some second trip echo. Little AP present.
16 May 2013	0.10	0.13	−0.15	0.40	Some passing showers and significant AP bloom after 0400 UTC, persisting through 1300 UTC.
20 May 2013	0.14	0.13	−0.09	0.47	Strong convection over radar early, followed by widespread stratiform. Significant AP in eastern quadrant late in the day.
2 Jun 2013	−0.03	0.13	−0.2	0.26	Clear air with minimal AP.

first. When that information is available, the $\mathrm{dB}Z95_{\mathrm{baseline}}$ value [see Eq. (1)] is subsequently adjusted to correspond to the absolute calibration. For example, if the $\mathrm{dB}Z95_{\mathrm{baseline}}$ value is 50 dBZ and independent calibration methods reveal a bias of −2 dB, then the new baseline becomes 52 dBZ. It is only when the absolute calibration is determined and the baseline adjusted that a *relative* calibration adjustment has definitive meaning. In this manner, the RCA is used as an invaluable tool to not only monitor relative changes but to make adjustments to keep calibration in check compared to independent methods.

One method of an independent calibration check is via the use of a self-consistency approach (Ryzhkov et al. 2005) when precipitation coverage is favorable: for example, fairly widespread moderate to heavy stratiform over a relatively large area. To compute the absolute reflectivity bias, the area–time integral of measured K_{DP} is calculated over a reflectivity range of Z_{min} (30 dBZ) to Z_{max} (48 dBZ). Then, the area–time integral of retrieved K_{DP} (as a function of Z_{H} and Z_{DR}) is calculated using the consistency principle. The Z_{H} bias is calculated as the adjustment (dB) needed for the integrals to match (Vivekanandan et al. 2003). This is done iteratively until the solution converges to within 0.1 dB. Self-consistency is one of the independent calibration methods used with the IFloodS dataset.

Another method employed to establish the absolute calibration baseline for the IFloodS dataset was the comparison of Z_{H} between NPOL and high-quality two-dimensional video disdrometer (2DVD) data. Disdrometer-based reflectivity was calculated from the observed drop size distribution using Raleigh scattering assumptions. Figure 5 shows the histogram and Gaussian fit of the difference in reflectivity (2DVD minus NPOL) from four disdrometers combined, and the NPOL RHI radar data above the instruments for the period from 3 May through 6 June 2013. The 0.9° elevation was chosen to mitigate blockage and sidelobe issues. The distance from NPOL to the disdrometers ranges from 15 to 69 km; therefore, the time it takes for rain to fall to each individual disdrometer differs. However, disdrometer data were selected 1 min later than NPOL scan times to allow the precipitation to fall to near ground level. The difference of approximately +2.15 dB indicates NPOL was lower than the combined disdrometers. Table 5 shows the difference between individual and combined disdrometers and NPOL from this significant portion of the IFloodS campaign. Differences from individual disdrometers range from +1.8 to +2.6 dB. All results imply NPOL reflectivity was lower relative to the disdrometer.

Based on the 2DVD reflectivity comparisons and several different adaptations of the self-consistency approach using different parameterizations and assumptions, it was decided that during IFloodS, NPOL was low by about 2.0 dB from 1 May 2013 through 6 June 2013, and low by 2.2 dB from 7 June 2013 through the end of

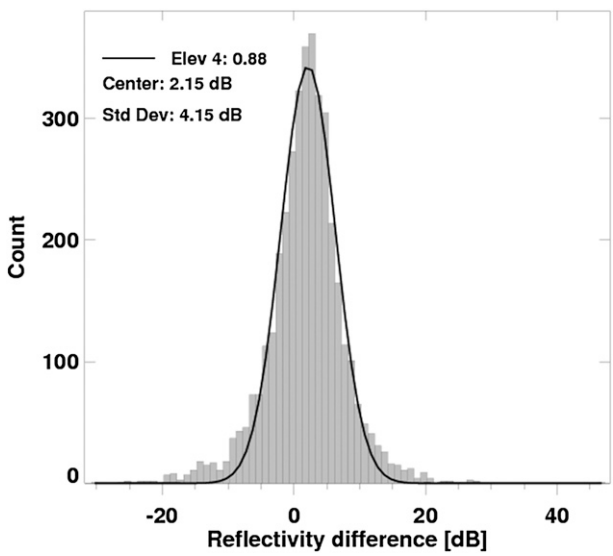

FIG. 5. Histogram and Gaussian fit of the reflectivity difference (2DVD minus NPOL) for the IFloodS period from 3 May through 6 Jun 2013 before calibration adjustment. The combined difference from four disdrometers and the extracted reflectivity above them near the 0.9° elevation level indicate NPOL reflectivity values were low by approximately 2.15 dB.

TABLE 5. Results from individual and combined 2DVD disdrometers from the IFloodS campaign showing the reflectivity difference (2DVD minus NPOL) near the 0.9° elevation level. The difference was determined as the center of the Gaussian fit of histogram data. Individual 2DVDs indicate that NPOL reflectivity is lower than the disdrometer within the range 1.8–2.6 dB. The combined result indicates 2.15 dB lower than the disdrometer. The instruments are named according to their serial number (SN).

Instrument	Range (km)	2DVD − NPOL (dB)
SN35	15.2	+1.93
SN36	24.5	+1.80
SN37	47.3	+2.61
SN38	69.2	+2.26
Combined		+2.15

the campaign on 15 June 2013. It is interesting to note that the slight increase of about 0.2 dB after 6 June 2013 has been tied to an issue with the polarization switches and is thought that the radar calibration was indeed altered. By adjusting the RCA baseline, the stability of the absolute reflectivity calibration is monitored over time. Figure 6 shows the RCA trace using the adjusted baseline and calibration-adjusted data for IFloodS. The legend in the top left shows the mean, standard deviation, minimum, and maximum daily RCA values over the entire campaign. In addition to IFloodS, the RCA technique has been successfully used to evaluate NPOL reflectivity from the MC3E (2011) and IPHEx (2014) field campaigns, and to adjust 16-plus years of data from the KPOL radar at Kwajalein Atoll (Marks et al. 2009).

5. Using the RCA to detect changes in the radar system

The RCA method can be used in near–real time to detect significant or even subtle changes in a radar system. As discussed, a change of 0.2 dB was detected with NPOL during IFloodS and was directly related to an engineering issue that affected calibration. However, not all RCA-detected changes are calibration related. Presented are two RCA case studies from the KPOL radar: one resulting in a subtle change due to antenna elevation and the other a significant change that affected power and calibration.

As described in Silberstein et al. (2008), antenna elevation changes result in RCA fluctuations, such that a 0.1° elevation change can result in an approximately 1-dB RCA change. During the most recent annual on-island KPOL calibration study in February 2014, the radar processor elevation offset was adjusted from −32.00° to −32.05° on the basis of careful measurement using a gunner's quadrant and sun calibration data (P. Smith 2013, personal communication). The adjustment of 0.05° corresponded to an RCA decrease of

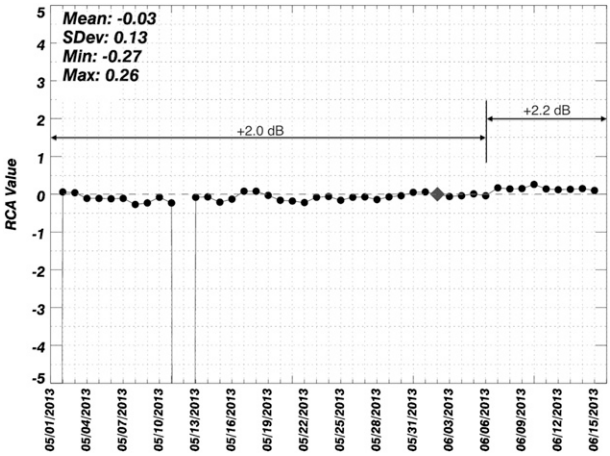

FIG. 6. Baseline-adjusted RCA trace (solid squares), along with original RCA trace for IFloodS. After careful consideration of comparisons between NPOL data and high-quality 2DVD data, as well as several self-consistency checks, it was determined that NPOL reflectivity was too low by 2.0 dB from 1 May 3 to 6 Jun 2013 and low by 2.2 dB from 7 to 15 Jun 2013. The legend in the top left shows the mean, standard deviation, minimum, and maximum daily RCA values over the entire campaign.

0.49 dB from 8 to 10 February. Although the magnitude of this change is close to the sensitivity boundary of the RCA method, it is clearly identifiable in the monthly RCA trace (Fig. 7a). The visible shift illustrates how sensitive the RCA method is to the scan elevation angle. Because the change is due to antenna elevation and not power, we know that an investigation into a potential calibration adjustment is not warranted.

Another case presents an example of how a component failure can result in a significant change to the day-to-day nominal state of the RCA statistics. In the course of daily operational monitoring of relative stability, a sudden RCA spike of approximately +4 dB was noticed on 31 December 2013 (Fig. 7b). The staff at both NASA Wallops Flight Facility (WFF) and Kwajalein were quickly in discussions to troubleshoot the issue. The on-island senior engineering technician identified the problem as a malfunctioning modulator, resulting in decreased pulse width and power. The decreased power is clearly visible as a positive jump in the RCA. The modulator was replaced the following week, and the RCA values dropped to their original state. Because the change in the RCA was due to a power issue, a calibration adjustment is warranted for this event.

6. Summary and future applications

This study explores the versatility of the RCA technique in application extension from KPOL to NPOL and possibly other radars. Results indicate that the RCA

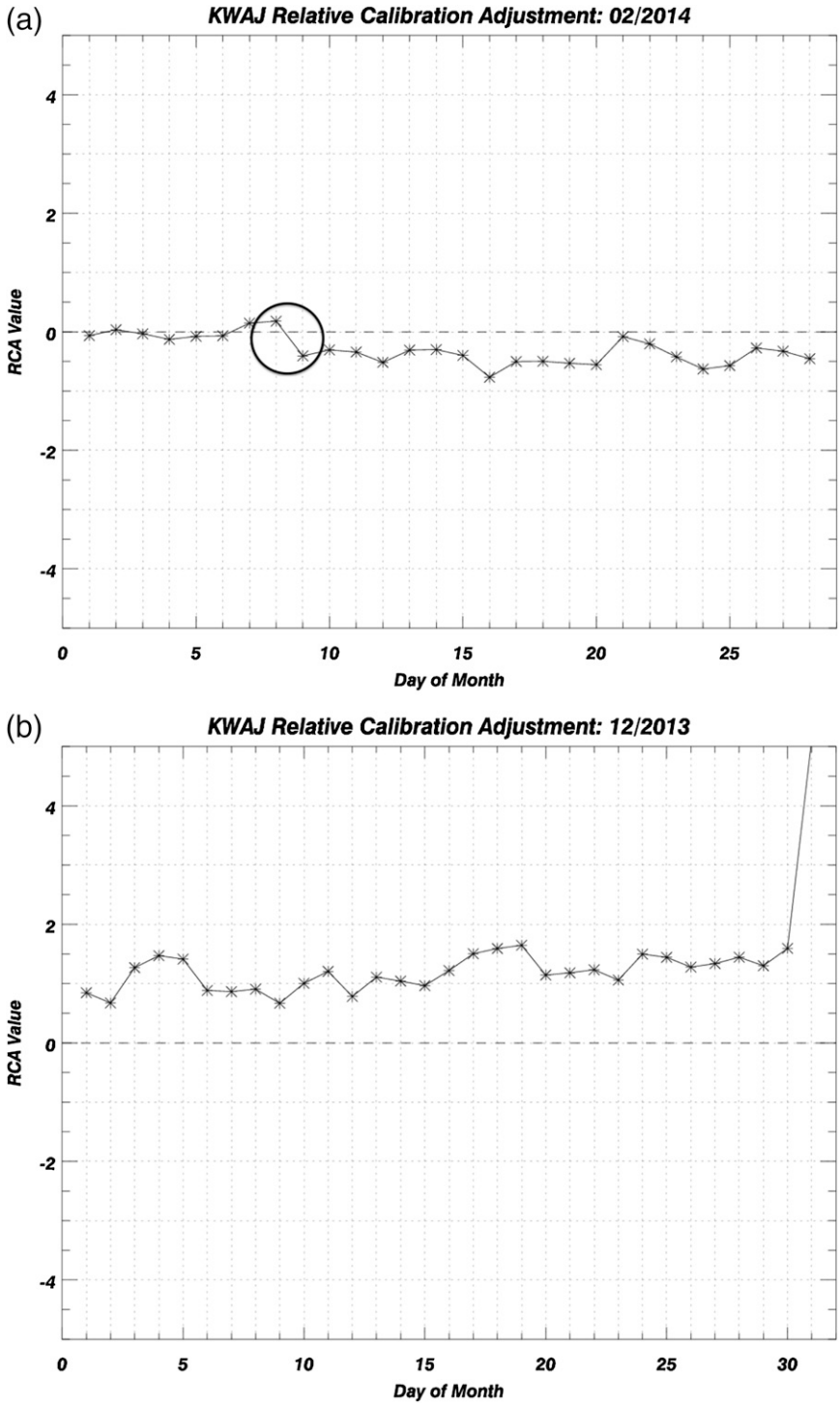

FIG. 7. (a) Monthly time series of daily RCA values for Kwajalein for February 2014. In this example, the radar processor elevation offset was adjusted from −32.00° to −32.05° on the basis of careful measurement using a gunner's quadrant and sun calibration data. The adjustment of 0.05° corresponded to an RCA decrease of 0.49 dB from 8 to 10 Feb, in keeping with results from Silberstein et al. (2008). (b) Monthly time series of daily RCA values for Kwajalein for December 2013. A large change detected on 31 Dec was tied to a malfunctioning modulator, resulting in decreased pulse width and power. The decreased power visibly resulted in a positive jump in the RCA on this date.

method was successfully extended to monitor and adjust reflectivity data during the IFloodS field campaign. To employ the method, it was shown that careful construction of a representative areal clutter map was necessary. The map was generated by determining the 1 km × 1° areas consistently in excess of a specified reflectivity threshold (55 dBZ for IFloodS). By limiting the range of the clutter map to within 1–5 km of the radar, neither precipitation nor anomalous propagation significantly affected the results. The calculation of the daily RCA values allows the user to detect even small changes in radar reflectivity calibration. In addition, when an absolute calibration baseline is established via sphere calibration, self-consistency, comparison to other instruments, or a myriad of other techniques, the technique can be used to adjust historical data and to monitor the stability of absolute calibration.

A benefit of the RCA is its ability to detect and adjust changes in the reflectivity data in a post hoc fashion. The RCA is being employed in a near-real-time operational environment with data from the KPOL radar to provide a stable calibration record for both TRMM/GPM GV efforts and operations of the U.S. Army's Reagan Test Site (RTS) weather station (Marks et al. 2009, 2011). The RCA method has also been successfully used to monitor the stability of the NPOL radar during the MC3E (2011) and IPHEx (2014) field campaigns and will be used in a future GPM field campaign [Olympic Mountains Ground Validation Experiment (OLYMPEX) in late 2015]. It is currently being used to track radar system stability and potential calibration changes during regular GV operations of NPOL at the GPM WFF Precipitation Research Facility.

It is certainly feasible that the RCA method may be successfully extended to other S-band surveillance ground-based radars (that do not filter ground clutter), thereby providing an invaluable and automated tool for maintaining high-quality radar data with relative calibration uncertainty of ±0.5–1.0 dB or better. Implications of this research extend beyond field experiments or any individual radar location. In the GPM era and beyond, calibration monitoring of ground-based radars will prove essential to effective validation of satellite retrievals and to the much broader radar and hydrology communities.

Acknowledgments. We thank the NASA PMM/GPM program. We acknowledge the myriad of contributions to our efforts from our recently deceased colleague, Dr. Arthur Hou. Also, we are grateful for the support of NASA management, specifically Drs. Ramesh Kakar (NASA/HQ), Scott Braun, and Matt Schwaller (NASA/GSFC), for their support of this research. We thank the NASA Wallops Field Support Office, especially Michael Watson, Nathan Gears, and Gary King, for their support and maintenance of the NPOL radar. Jason Pippitt of the TRMM/GPM Ground Validation Office performed data processing, analysis, and quality control of the NPOL IFloodS and KPOL datasets.

REFERENCES

Atlas, D., and S. C. Mossop, 1960: Calibration of a weather radar by using a standard target. *Bull. Amer. Meteor. Soc.,* **41,** 377–382.

Billingsley, J. B., 1993: Ground clutter measurements for surface-sited radar. MIT Lincoln Laboratory Tech. Rep. 786, Revision 1, 81 pp.

——, and J. F. Larrabee, 1991: Multifrequency measurements of radar ground clutter at 42 sites. MIT Lincoln Laboratory Tech. Rep. 916, Vol. 1, 251 pp.

Gerlach, J., and W. A. Petersen, 2011: NPOL: The NASA transportable S-band dual-polarimetric radar. Antenna system upgrades, performance and deployment during MC3E. *35th Conf. on Radar Meteorology,* Pittsburgh, PA, Amer. Meteor. Soc., 192. [Available online at https://ams.confex.com/ams/35Radar/webprogram/Paper191918.html.]

Jensen, M. P., and Coauthors, 2010: Midlatitude Continental Convective Clouds Experiment (MC3E). DOE Tech. Rep. DOE/SC-ARM/10-004, 31 pp.

Marks, D. A., D. B. Wolff, D. S. Silberstein, A. Tokay, J. L. Pippitt, and J. Wang, 2009: Availability of high-quality TRMM ground validation data from Kwajalein, RMI: A practical application of the relative calibration adjustment technique. *J. Atmos. Oceanic Technol.,* **26,** 413–429, doi:10.1175/2008JTECHA1174.1.

——, ——, L. D. Carey, and A. Tokay, 2011: Quality control and calibration of the dual-polarization radar at Kwajalein, RMI. *J. Atmos. Oceanic Technol.,* **28,** 181–196, doi:10.1175/2010JTECHA1462.1.

Rinehart, R. E., 1978: On the use of ground return targets for radar reflectivity calibration checks. *J. Appl. Meteor.,* **17,** 1342–1350, doi:10.1175/1520-0450(1978)017<1342:OTUOGR>2.0.CO;2.

Ryzhkov, A. V., and D. S. Zrnic, 1998: Polarimetric rainfall estimation in the presence of anomalous propagation. *J. Atmos. Oceanic Technol.,* **15,** 1320–1330, doi:10.1175/1520-0426(1998)015<1320:PREITP>2.0.CO;2.

——, S. E. Giangrande, V. M. Melnikov, and T. J. Schuur, 2005: Calibration issues of dual-polarization radar measurements. *J. Atmos. Oceanic Technol.,* **22,** 1138–1154, doi:10.1175/JTECH1772.1.

Silberstein, D. S., D. B. Wolff, D. A. Marks, D. Atlas, and J. L. Pippitt, 2008: Ground clutter as a monitor of radar stability at Kwajalein, RMI. *J. Atmos. Oceanic Technol.,* **25,** 2037–2045, doi:10.1175/2008JTECHA1063.1.

Skolnik, M., 2001: *Introduction to Radar Systems.* McGraw-Hill, 772 pp.

Vivekanandan, J., G. Zhang, S. Ellis, D. Rajopadhyaya, and S. Avery, 2003: Radar reflectivity calibration using differential propagation phase measurement. *Radio Sci.,* **38,** 8049, doi:10.1029/2002RS002676.